Contents lists available at ScienceDirect

Renewable Energy

journal homepage: www.elsevier.com

Modelling assessment of the tidal stream resource in the Ria of Ferrol (Nw Spain) using a year-long simulation

Marc Mestres[a, b, *], Pablo Cerralbo[a, b], Manel Grifoll[b], Joan Pau Sierra[a, b], Manuel Espino[a, b]

[a] International Centre for Coastal Resources Research (CIIRC), c/ Jordi Girona 1-3, Mòdul D1, 08034 Barcelona, Spain
[b] Laboratori d'Enginyeria Marítima (LIM-UPC), Universitat Politècnica de Catalunya-BarcelonaTech, c/ Jordi Girona 1-3, Mòdul D1, 08034 Barcelona, Spain

ARTICLE INFO

Article history:
Received 8 May 2017
Received in revised form 9 July 2018
Accepted 21 July 2018
Available online xxx

Keywords:
Ría of Ferrol
Tidal current energy
Tidal resources
Numerical modelling
ROMS

ABSTRACT

The availability of tidal stream energy in the Ría of Ferrol (NW Spain) has been assessed using a long term hydrodynamic simulation (351 days). A priori, a strait in the central part of the estuary seems a promising site for tidal energy tapping, but the results show that barotropic currents rarely exceed 0.9 m/s during spring tides, with a maximum peak power density of 0.45 kW/m^2 estimated at a spring tide mid-ebb. The maximum annual energy density is estimated at 415 kWh/m^2, significantly lower than at other nearby estuaries. A comparison of the annual resource estimates shows that differences of up to 35% can be introduced depending on whether a simulation of one tidal cycle, one lunar month, or a full year is used for the calculations. This proves that usual tidal resource estimations, based on a single tidal cycle, can significantly misestimate the tidal energy potential of a site.

© 2018.

1. Introduction

The energetic demands of the planet are continuously growing due to the increase in population and the emergence of new energy-demanding activities [1]. In addition, the depletion of fossil fuel reserves [2] and the rising awareness of the impact of fossil fuels on climate change [3] have increased the interest for the exploitation of renewable energy sources [4]. Amongst them, tidal current energy is one of the most promising [2,5,6] due to several advantages with respect to other renewable energy sources: a) the high predictability of tidal currents when compared to atmospheric flows, b) the higher density of seawater (over 800 times that of air) assuring much larger energy available for a tidal energy converter (TEC) than for a wind turbine under similar conditions [7], c) the minimum environmental impact compared to tidal barrage facilities [6] and d) the absence of extreme flow velocities that might damage the equipment or complicate its maintenance [6], although this depends strongly on the flow profiles induced by the local bathymetry near the TEC deployment site [8]. As a negative aspect, the extraction of tidal energy reduces flow speed [9] and can lead to modifications in the dispersion and transport patterns and, therefore, changes in the local water quality [10], sediment patterns [11] or even in the wave energy regime, depending on the particular wave-current interaction [12].

On the other hand, in 2009 the EU adopted the directive 2009/28/EC, which stipulates that by 2020 at least 20% of the final EU-wide energy consumption must be obtained from renewable sources [13]. To achieve this goal, renewable energies have been boosted in the past few years in European countries, increasing their share of gross energy consumption from 5% in 1999 to 17% in 2016 [14]. In the particular case of Spain, renewable sources account for 17.3% of the gross consumption, more than doubling the percentage in 2004 (8.5%, [14]). About 90% of the *green* electricity generated is provided by wind, hydraulic and solar sources [7]. Nevertheless, in the last few years the interest in marine energies has increased considerably due to their large potential as well as being seen as an opportunity for helping to achieve the EU directive goals. Although most of this interest has been focused on wave energy resources (e.g., [15–17]), tidal stream energy has also been considered for generating electric power.

In order for tidal stream technology to be economically viable, sufficient current velocities are needed. Therefore, detailed resource assessments are required in advance of device deployments to determine their commercial feasibility [18]. In recent years, many studies have been undertaken to evaluate tidal current energy resources at different coastal locations, using either extensive field campaigns or numerical modelling. Some examples include the UK [19–21], USA [22,23], Canada [24], Norway [25], Portugal [26], China [27], Korea [28], Indonesia [29] and Iran [30].

One of the areas with a high tidal current energy potential is the mesotidal Spanish Atlantic Coast, with spring tides of up to 4 m. In particular, Spain's north-western (NW) coast is characterized by the presence of several estuaries (rías) with large tidal prisms. The significant tidal volumes combined with the shape of the estuaries can produce strong tidal currents in certain areas, which could be harvested to

* Corresponding author. International Centre for Coastal Resources Research (CIIRC), c/ Jordi Girona 1-3, Mòdul D1, 08034 Barcelona, Spain.
Email addresses: mmestresridge@gmail.com (M. Mestres); pablo.cerralbo@upc.edu (P. Cerralbo); manel.grifoll@upc.edu (M. Grifoll); joan.pau.sierra@upc.edu (J.P. Sierra); manuel.espino@upc.edu (M. Espino)

https://doi.org/10.1016/j.renene.2018.07.105
0960-1481/ © 2018.

UNCORRECTED PROOF

produce electric power. For these reasons, several studies have assessed the tidal resource at different locations in this region [6,7,31,32].

The objective of this paper is to assess the energetic potential of the tidal stream around the Ría of Ferrol based on the results of a quasi year-long numerical simulation using a three-dimensional (3D) hydrodynamic model. The analysis aims to identify the areas in which the available tidal energy is largest and, eventually, the most appropriate theoretical locations for the deployment of TECs. The study also compares the results obtained using a near year-long data with those found from more common approaches (i.e., using only data corresponding to a lunar month or a tidal cycle). This represents a step forward in the methodological perspective of these analyses.

2. Site description

The Ría of Ferrol is located in the NW Spanish coast (Fig. 1), between 43°27′ and 43°30′N and between 8°9′ and 8°21′W [33]. It is one of the 18 Galician rías, coastal inlets formed by the partial submergence of unglaciated river valleys. This ría is 15 km long, extends over a 21 km^2 area and has a volume that ranges from 0.21 km^3 at low tide to 0.29 km^3 at high tide [34]. The water exchange with the shelf takes place through the Ferrol Strait, a 2 km long and narrow (0.35 km) channel, with a mean depth of 20 m. At the head of the estuary, the Xubia and Belelle rivers represent the main freshwater input to the ría, although in modest quantities. Their combined mean annual input is about 6.3 m^3/s [35], with minimum outflows in late summer (1 m^3/s in August and September) and maxima in February (15 m^3/s).

The ría is mesotidal and semidiurnal, with tidal amplitudes between 1.5 m at neap tides and 4 m during spring tides [34]. Tidal forcing is the main mechanism driving the exchange of water between the ría and the shelf [35], whereas the residual circulation is mostly controlled by wind forcing, given the low river inflow [33]. Previous studies [33,34] have shown that currents within the ría can exceed 1 m/s in some areas.

The estuary can be divided into four different stretches [33]: the outermost estuary mouth, between Cape Prioriño Chico and Cape Coitelada, 2.2 km wide and a depth of about 33 m; the Ferrol Strait, extending up to Cape Leiras; the middle part of the estuary, up to As Pias bridge, 2.3 km wide and 15 m deep, and hosting the Ferrol city and harbour; and the innermost shallow area, with extensive mudflats at low tide [34]. This latter part is not considered in this study.

3. Methodology

The tidal stream energy resource in the Ría of Ferrol is estimated from the barotropic flows obtained from a 351-day long simulation using a 3D implementation of the ROMS system (Regional Ocean Modelling System, [36]). By using a long time series, it is expected to smooth out and quantify the variations in the tidal resource assessment that arise when shorter representative time windows (e.g., 14-day tidal cycles, or 28-day lunar months) are adopted. Previous studies comparing these shorter time periods [7,28] have shown that the potential tidal stream energy in an area can be under- or overestimated by as much as 16%, depending on whether the considered tidal cycle corresponded to a perigean or an apogean tide.

a) The numerical model

The ROMS code is a 3D, free-surface, terrain-following numerical model that solves the Reynolds-averaged Navier-Stokes equations using the hydrostatic and Boussinesq assumptions [36]. ROMS uses the Arakawa-C differencing scheme to discretize the horizontal grid in curvilinear orthogonal coordinates, and finite difference approximations on vertical stretched coordinates [37]. The model follows a split-explicit approach in which the evolution of the barotropic (i.e., free surface and 2DH velocities) and baroclinic (temperature, salinity and 3D momentum) terms are solved separately, using different time steps. This technique considerably reduces the duration of the simulations, without affecting the validity of the solutions. The numerical details of ROMS are described extensively in Ref. [36].

The implementation of the model in the Ría of Ferrol, developed within the framework of the SAMOA project [38], is based on a regular grid with a spatial resolution of approximately 70 m in both latitudinal and longitudinal directions, and 15 sigma levels in the vertical direction. This grid is one-way nested within a parent grid (350 m × 350 m x 20 sigma-levels) which, in turn, is nested into the Iberia-Biscay-Ireland (IBI) domain of the EU operational system provided by Copernicus Marine Services [39]. Hourly barotropic water currents and sea levels supplied by IBI-Marine and Forecasting Centre (IBI-MFC) are accommodated to the open boundaries of the Ferrol parent grid domain consistently with Chapman and Flather algorithms [40]. The baroclinic component of the water flows, temperature and salinity are imposed from IBI-MFC daily average values. At the head of the ría, the freshwater input from the river Jubia is introduced through a climatic run-off value and a constant salinity of 18. High-resolution (5 km) atmospheric forcing, including wind speed, atmospheric

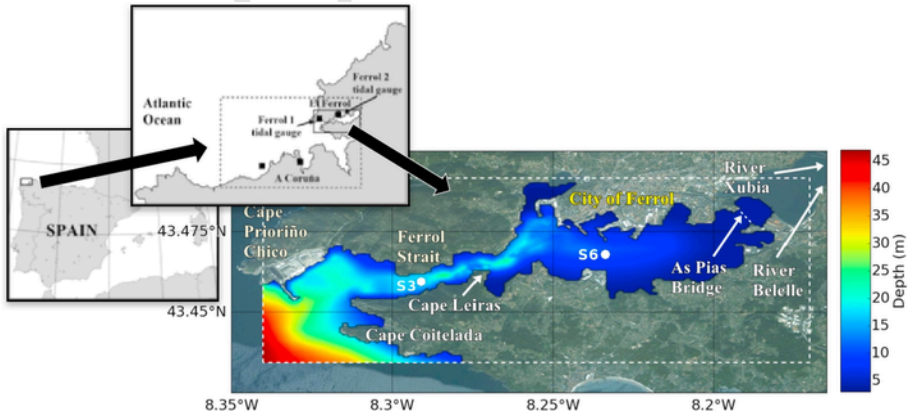

Fig. 1. The Ría of Ferrol. The larger figure shows the bathymetry of the study area, with the local computational domain used for the analysis in this study specified by the dashed line. S3 and S6 mark the position of the current meters used for model validation, and black filled squares in the central panel show the position of the tidal gauges.

CORRECTED PROOF

pressure and surface net heat and salinity fluxes, is provided by the Spanish Meteorological Agency (AEMET).

The bottom boundary layer is parameterized with a logarithmic profile using a characteristic bottom roughness height of 0.002 m. The turbulence closure scheme for the vertical mixing is the generic length scale (GLS) tuned to behave as a k-epsilon [41]. Horizontal harmonic mixing of momentum is defined with constant values of 5 m^2/s.

The model has been run to simulate the oceanographic conditions in the ría between 7 January 2014 and 25 December 2014, i.e., during 351 days, providing hourly information on the sea level, vertically-integrated and 3D currents, and 3D salinity and water temperature values. The salinity and water temperature distributions have been combined to derive 2DH density values.

b) Estimation of the potential tidal stream energy

The maximum power potentially available to a tidal energy converter is defined as the kinetic energy of a fluid in a stream tube with a diameter equal to that of the turbine rotor, i.e.,

$$P(x,y) = \frac{1}{2}\rho(x,y)\cdot A\cdot V(x,y)^3 \quad (1)$$

where P is the total power available to the TEC at position (x,y), ρ is the density of the fluid, A is the cross-sectional area of the TEC's rotor blades and V is the flow velocity averaged over this area. This equation is dependent on the characteristics of the TEC, and is thus not useful for the generic assessment of tidal energy availability at a given location. To avoid this dependency, the average power density (APD), defined as the power per unit area averaged over a representative time period, is introduced.

$$APD(x,y) = \frac{1}{2}\frac{1}{N}\sum_{i=1}^{N}\rho(x,y)\cdot V_i(x,y)^3 \quad (2)$$

where V_i (i=1, …, N) is the velocity of the current at time t_i, and N is the number of data values within the representative period chosen. Here it is assumed that the current field is given by a discrete time-series, either from field measurements or numerical simulations. For this study, V is the vertically-averaged current every hour at each computational node; the use of a 2DH velocity field in this case is acceptable since the flow is relatively uniform through the water column, with maximum values in the surface layers induced by wind forcing.

However, it must be taken into account that not all of the tidal power predicted by equations (1) and (2) can be effectively extracted, since part of the energy is lost during the transformation process. This is considered for by correcting the previous equations with a power coefficient (C_p) to yield the effective output power provided by a TEC. Equation (2) then becomes

$$APD(x,y) = C_p\frac{1}{2}\frac{1}{N}\sum_{i=1}^{N}\rho(x,y)\cdot V_i(x,y)^3 \quad (3)$$

This coefficient accounts for the power losses during the transformation process associated to factors such as the variability of the incident flow speed, the type of turbine (i.e. vertical or horizontal axis turbine), the pitch angle of its blades [42], its relative position within an array of turbines [43], and the overall mechanical efficiency of the TEC. Its accepted values range between 0.3 and 0.5 [44,45], but might increase up to Betz's limit (0.59) or even beyond [45] under certain conditions.

For the goal of this paper, which is the simple resource assessment of a specific coastal area, the power coefficient can be equaled to 1.

4. Results and discussion

The performance of the numerical model has been validated for the entire simulation period by comparing the simulated sea level data with observations recorded by four tidal gauges in the parent domain (see Fig. 1). Fig. 2 shows this comparison at two points within the ría itself for a spring and a neap tide. The agreement for both cases is very close, with correlation values R of 0.99 and root-mean-square errors (RMSE) of around 6–7 cm for the spring tide, and about 3 cm for the neap tide. Overall, the correlation and RMSE values for the full 351-day time series are larger than 0.99 and smaller than 3 cm, respectively, showing the accuracy of the modelled sea level.

On the other hand, and regarding the temperature, salinity and current data, the lack of observational temporal series in the area coincident with the simulation period does not allow a direct quantitative validation of the model results, but a qualitative comparison can be done with previous studies. For instance, deCastro [33] measured currents in the narrowest part of the ría (43.465°N, 8.2833°W) using a Doppler current meter, and again used current meters at two stations (S3 and S6, see Fig. 1) in Ref. [34] to analyse different aspects of the ría's hydrodynamics. The modelled results obtained in this study are comparable with their measured data, both in magnitude and general behavior at the observational stations, considering the different time frames. Thus, axial currents at the computational node closest to the measuring station in Ref. [33], in the Ferrol strait, present magnitudes at mid- and bottom layers comparable to their field measurements (see Fig. 3 in Ref. [33]) for a period with a similar tidal range (maxima around 0.5 m/s at mid-depth, and smaller for deeper waters). Currents near the surface are not comparable, since they are very influenced by the prevailing winds. Moreover, deCastro [34] presents along-axis root-mean-square velocities measured at two stations inside the ría, averaged over depth and tidal cycle (U_{rms}), and shows that they are linearly related to the tidal range, independent of the wind and density conditions. The same procedure with the data modelled in this study replicates the linear relationship between U_{rms} and the tidal range, but with slightly different U_{rms} values (Table 1). The physical alteration of the estuary since deCastro's field campaings - which include periodic dredging, the construction of the outer Ferrol harbour at the ría mouth, or the expansion of the Mugardos harbour facilities, on the southern bank near S6- makes it difficult to perform a direct comparison between deCastro's data and the modelled currents, but both the values and trends indicate that the tidal flow is adequately reproduced inside the ría.

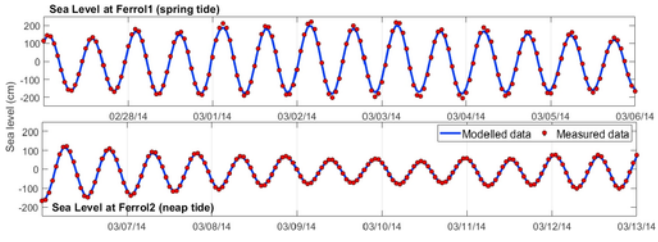

Fig. 2. Comparison between sea level measurements (red circles) and the modelled values (blue line) at two tidal gauges within the Ría of Ferrol during a spring (top) and a neap tide (bottom) in February–March 2014.

UNCORRECTED PROOF

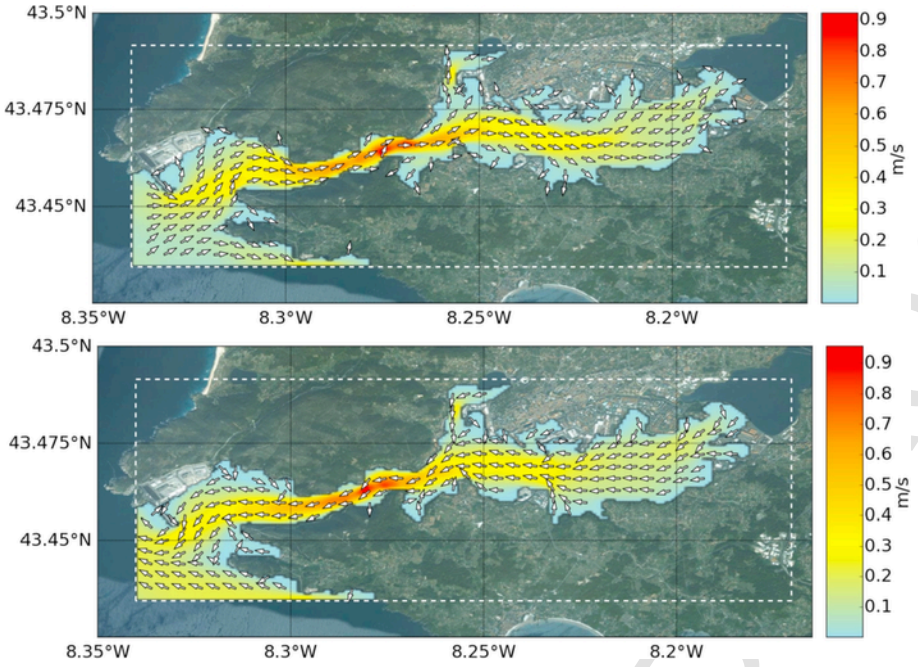

Fig. 3. Depth-averaged currents in the Ría of Ferrol at mid-flood (top) and mid-ebb (bottom) during a spring tide.

Table 1
Tidal range *vs.* U_{rms} at two positions in the Ría of Ferrol, modified from Ref. [34].

Tidal range (m)	U_{rms} (m/s) [34]	U_{rms} (m/s) modelled		
		Minimum	Mean	Maximum
Strait of Ferrol (S3)				
3.5	**0.50**	0.40	**0.41**	0.42
3.2	**0.47**	0.37	**0.39**	0.41
2.6	**0.39**	0.30	**0.34**	0.39
2.3	**0.32**	0.26	**0.31**	0.41
1.8	**0.25**	0.20	**0.27**	0.36
1.5	**0.17**	0.16	**0.26**	0.39
Middle station (S6)				
3.6	**0.11**	0.20	**0.20**	0.21
2.8	**0.10**	0.15	**0.16**	0.20
2.5	**0.09**	0.12	**0.15**	0.19

The results from the numerical model reveal a vertically-averaged (2DH) circulation pattern typical of tidally-dominated estuaries, with a clear up- and down-stream circulation associated to the flood and ebb tide, and water recirculation in the numerous lateral inlets. An area with higher velocities is located inside the ría, approximately 3 km upstream from the estuary mouth, coinciding with the narrowing of the channel, as shown in Fig. 3. Here, the barotropic current at both mid-flow (top) and mid-ebb (bottom) of the 2 March 2014 spring tide show maxima in the same area around the Ferrol Strait. The largest current speeds are 0.92 m/s and 0.95 m/s during the flood and the ebb, respectively, and are obtained at different locations, separated by about 420 m. Fig. 4 shows the time evolution of the 2DH flow velocity at this point of mid-ebb current maximum (P2) during 2014, together with the histogram of the annual modelled velocity distributions at both the mid-flood (left, P1) and mid-ebb (right, P2) maxima locations. In general, the mean maximum speed during the 2014 spring tides at P2 is around 0.90 m/s, whereas it is only 0.70 m/s during neap tides. Both values are smaller than those proposed by Refs. [19] and [46] as the thresholds above which the tidal stream power is worth exploiting under current technological conditions.

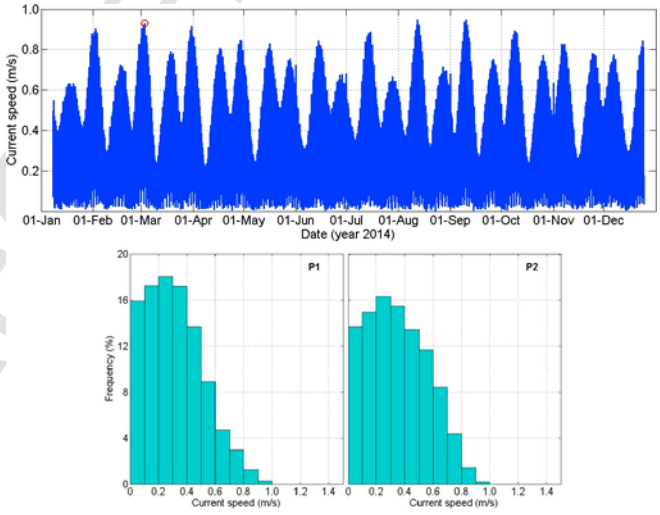

Fig. 4. Top) 2DH Current speed modelled at the location of highest velocities in the ría in 2014. The red circle marks the spring tide used for Fig. 5. Bottom) Histogram of modelled velocity yearly distribution at the positions of maximum mid-flood (left) and mid-ebb (right) velocities.

The spatial distribution of power density during the spring tide of 2 March 2014 is shown in Fig. 5 for both mid-flood (top) and mid-ebb (bottom). Power maxima are found in similar areas for both tidal phases. For the mid-flood power density distribution, maximum power density is found at P1; for the mid-ebb density, the maximum is found at P2. As expected, the mid-ebb power for this spring tide is larger than the mid-flood power (0.45 kW/m^2 *vs.* 0.40 kW/m^2). In both cases, the power density values are considerably smaller than those found in other Galician rías: Vigo (7.5 and 5.6 kW/m^2, for the mid-flood and mid-ebb, respectively [7]), Muros (5 - 2 kW/m^2 [31]), or Ortigueira (8–6 kW/m^2 [6]).

The 2DH average power density during the full simulated period can be calculated from equation (2) using the flow speed time series at

UNCORRECTED PROOF

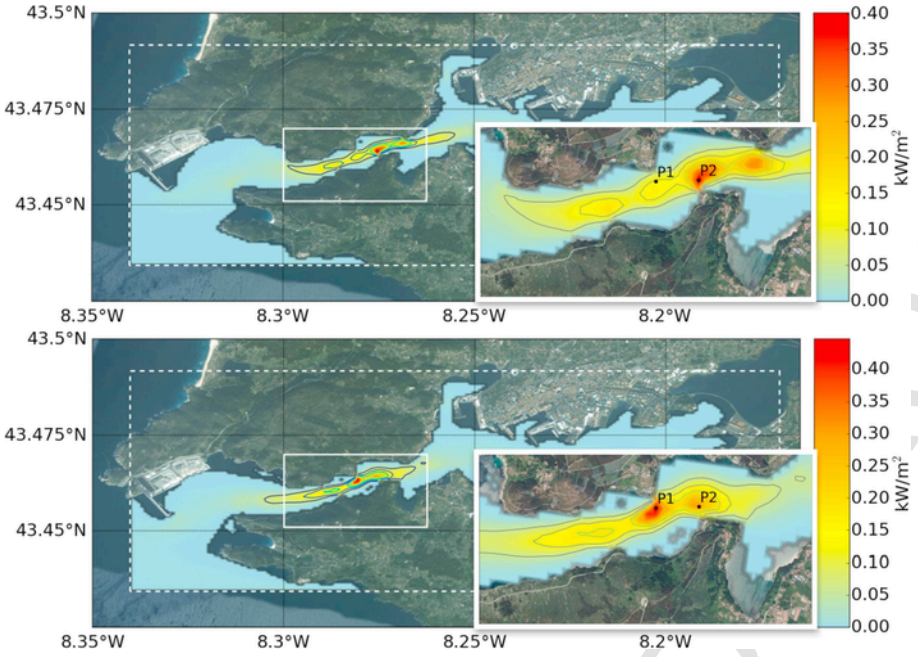

Fig. 5. 2DH power density in the domain at mid-flood (top) and mid-ebb (bottom) during the 2 March 2014 spring tide. The area of highest values in the Ferrol strait is enlarged.

each computational node. The resulting distribution is shown in Fig. 6. The highest hourly APD within the ría is 0.047 kW/m^2, obtained at the position of maximum mid-ebb power density (P2), yielding an annual energy density of 411.84 kWh/m^2.

On the other hand, the time variation of the power density at P2, obtained from the current series presented in Fig. 4 is shown in Fig. 7. The area under the power density curve is an estimation of the total energy available for extraction throughout the simulated period; at P2, the density of available energy is 399.14 kWh/m^2 during the 351 simulated days. By extrapolating, the annual energy density is found to be 415.33 kWh/m^2, which is almost the same as the value (411.84 kWh/m^2) obtained previously from considering the hourly APD. These results show that, in the Ría of Ferrol, the available energy associated to the tidal stream is considerably lower than the tidal energetic potential of other Galician rías, such as the Ría of Muros (5.3 MWh/m^2 [31]) or the Ría of Vigo (14.64 MWh/m^2 [7]).

Two comments can be done regarding these estimates. First, the current velocity provided by the numerical model corresponds to the flow speed averaged over the area of the computational grid cell (70×70 m^2). This implies that sub-grid velocities will occasionally be higher than the mean values, thus leading to a potential underestimation of the energy content available for extraction, particularly when the grid resolution is larger than typical TEC dimensions. Nevertheless, the numerical output used herein compares positively with pointwise current measurements, suggesting that it is indeed representative of the flow in the Ría.

Second, the procedure followed in the literature to assess the yearly energy resource at a specific location is based usually on evaluating this resource for a reduced time period, and then extrapolating to obtain the annual estimation. Typically, this time window corresponds to the approximately 14-day long spring-neap tidal cycle (e.g., [16,19,20,31,47]). However [28], found that such a short period ignored the fact that the Earth-Moon distance varies during a lunar month, and proposed using 28-day simulations. In their study, they determined that the difference between using 14- or 28-day simulations could represent around a 12% mis-estimation of the tidal energy resource off Korea, a figure comparable with the 16% difference found by Ref. [7] in Vigo (Spain).

Nevertheless, the time series of water flow velocity and power density given in Figs. 4 and 7 suggest that neither options are adequate solutions to compute the annual energy availability. Both plots show significant divergences in signal amplitude between different tidal cycles,

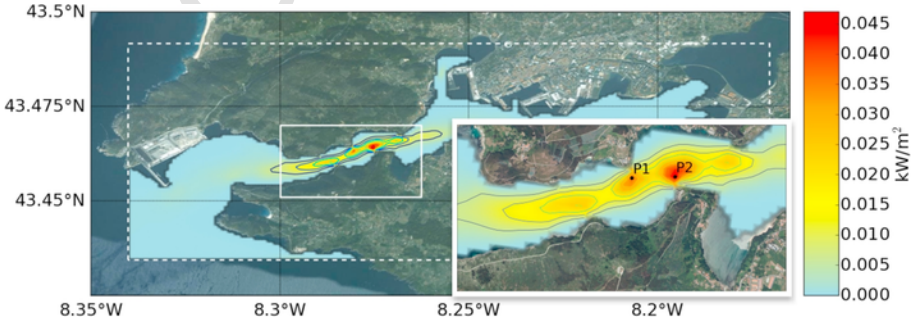

Fig. 6. 2DH yearly averaged power density (APD) in the Ría of Ferrol, during 2014. The area of highest APD values in the Ferrol strait is enlarged.

CORRECTED PROOF

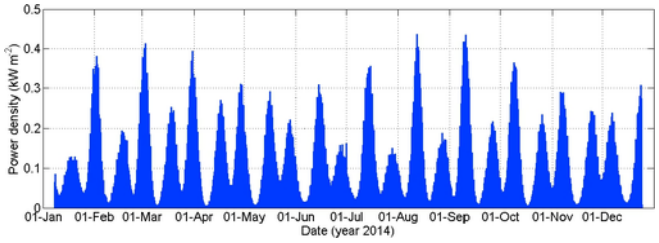

Fig. 7. Vertically-averaged power density at P2 during the simulation period (7 January–25 December 2014).

which will eventually lead to a disparity in the resource estimation. At P2, for instance, the instantaneous power density corresponding to the maximum perigean spring tide current is 0.44 kW/m^2 (Fig. 7), over three times larger than the power density associated to the weakest apogean spring tide current (0.13 kW/m^2).

Taking advantage of the long time series available for this study, it is possible to evaluate the error incurred in the assessment of annual tidal stream resource when smaller integration periods are considered. For this, the average power density at P2 is calculated for each tidal cycle (14 days), and from here the lunar month (28 days) and total (351 days) APDs are obtained. Following the common procedure, each APD is conveniently multiplied to yield the corresponding annual energy density (Fig. 8).

In the particular case of the Ría of Ferrol, it can be seen that the selection of the tidal cycle and of the length of the averaging period for the APD has an important effect on the final estimation of yearly tidal stream resource. As an example, using the modelled tidal currents for March and computing the APD from the first (perigean) and second (apogean) tidal cycles yields an annual energy resource of 558.0 kWh/m^2 and 374.3 kWh/m^2, respectively; using the full lunar month the estimate is 466.1 kWh/m^2. Thus, a resource analysis based on the March 2014 perigean tidal cycle would have overestimated the annual energy availability by 34% as compared to using the complete yearly simulation, whereas the extrapolation of the apogean tidal cycle would have been underestimating the resource by 10%. On the other hand, consideration of this specific lunar month provides a yearly resource evaluation 12% larger than that obtained from the annual data series.

Overall, depending on the integration period the estimated tidal stream resource for 2014 can vary between 264.9 kWh/m^2 and 562.8 kWh/m^2 if the 14-day tidal cycle is used to compute the APD and between 368.1 kWh/m^2 and 466.1 kWh/m^2 when the lunar month is considered. In relation to the APD obtained from the full 351-day series, this corresponds to a ±36% deviation for the tidal cycle data, and between −11% and +12% for the lunar month data. The latter misestimates are comparable with those found previously by Ref. [28] in Korea and [7] in the Ría of Vigo using a lunar month, which were between 12 and 16%. This highlights the importance of using a long time series to evaluate tidal stream resources, and indicates that previous assessments based on data from only one or two tidal cycles are not sufficiently accurate.

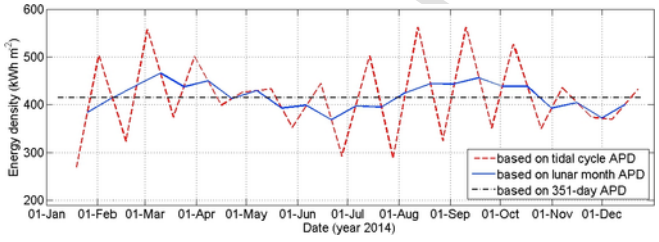

Fig. 8. Annual energy density at P2, at different times, estimated using APDs calculated using different integration periods.

5. Conclusions

The energy potentially available in the Ría of Ferrol tidal stream has been quantified using the results of a one year long 3D hydrodynamic numerical simulation. The model implemented in this region is based on a 3-level nesting scheme developed within the SAMOA project, originally fed by the Copernicus IBI data, and has been positively validated in a quantitative manner using measured sea levels, and qualitatively by comparing the modelled currents to field measurements provided in previous studies by other authors. Because of the particular characteristics of the Ría, which is relatively shallow and acts as a navigational pathway to Ferrol harbour, only its energetic *content* has been assessed, and no attempt has been done to evaluate its possible energetic *output* using current-technology TEC's.

The analysis of the model output indicates that only in the narrowest part of the estuary, the Ferrol Strait, does the 2DH current speed approach the 1.0 m/s threshold proposed by Ref. [47] for the flow to contain sufficient energy to be harnessed by present technology TEC's. During the flood phase, flow velocities are slightly smaller than during the ebb. In terms of power density, the mid-ebb spring tide contains up to 0.45 kW/m^2 at the position of strongest currents (P2 in the text), whereas the mid-flood can provide up to 0.40 kW/m^2. The maximum average power density for the complete simulated period is around 0.047 kW/m^2, i.e., significantly smaller than that obtained at other nearby rías.

As a consequence, the annual energy density at this position is also lower than in other Galician rías. At P2, the maximum value is around 415 kWh/m^2, which is one thirteenth of that estimated in the Ría of Muros (5.3 MWh/m^2), and over 35 times smaller than the energy density in Vigo (14.7 MWh/m^2). The values found are an indication of the limited viability of this ría as a source of tidally generated power under actual TEC design.

However, previous studies in other rías have used short time windows (tidal cycle or lunar month) to compute the APD, which was then extrapolated to obtain an annual value of the energy density. This work has shown that, following such an approach instead of using longer (annual) time series, can introduce large errors (up to ±35%) in the estimation of the annual energy content. This implies, first, that tidal energy resource estimates obtained from short integration periods might not accurately reflect the energy content of the tides and, second, that estimations from studies using integration windows of different lengths are not directly comparable.

Acknowledgements

The implementation of the hydrodynamic numerical model in Ferrol is part of the SAMOA Project, co-funded and led by the Spanish National Harbour Authority (Puertos del Estado). The support of the Secretaria d'Universitats i Recerca of the Dpt. d'Economia i Coneixement de la Generalitat de Catalunya (Ref. 2014SGR1253) is also acknowledged.

References

[1] J.P. Sierra, C. Martín, C. Mösso, M. Mestres, R. Jebbad, Wave energy potential along the Atlantic coast of Morocco, Renew. Energy 96 (2016) 20–32.
[2] F. O'Rourke, F. Boyle, A. Reynolds, Tidal energy update 2009, Appl. Energy 87 (2010) 398–409.
[3] IPCC, in: Core Writing Team, R.K. Pachauri, L.A. Meyer (Eds.), Climate Change 2014: Synthesis Report. Contribution of Working Groups I, II and

UNCORRECTED PROOF

III to the Fifth Assessment Report of the Intergovernmental Panel on Climate Change, IPCC, Geneva, Switzerland, 2014, 151 pp..
[4] M. Mestres, M. Griñó, J.P. Sierra, C. Mösso, Analysis of the optimal deployment location for tidal energy converters in the mesotidal Ría de Vigo (NW Spain), Energy 115 (2016) 1179–1187.
[5] C.M. Johnstone, K. Nielsen, T. Lewis, A. Sarmento, G. Lemonis, EC FPVI coordinated action on ocean energy: a European platform for sharing technical information and research outcomes in wave and tidal energy systems, Renew. Energy 31 (2006) 191–196.
[6] G. Iglesias, M. Sánchez, R. Carballo, H. Fernández, The TSE Index – a new tool for selecting tidal stream sites, Renew. Energy 48 (2012) 350–357.
[7] M. Mestres, M. Griñó, J.P. Sierra, C. Mösso, Quantification of the tidal stream exergy in the Ría de Vigo (NW Spain), Int. J. Exergy 23 (2017) 47–62.
[8] P. Evans, A. Mason-Jones, C. Wilson, C. Wooldridge, T. O'Doherty, D. O'Doherty, Constraints on extractable power from energetic tidal straits, Renew. Energy 81 (2015) 707–722.
[9] R. Vennell, Realizing the potential of tidal currents and the efficiency of turbine farms in a channel, Renew. Energy 47 (2012) 95–102.
[10] R. Ahmadian, R. Falconer, B. Bockelmann-Evans, Far-field modelling of the hydro-environmental impact of tidal stream turbines, Renew. Energy 38 (2012) 107–116.
[11] R. Ahmadian, R. Falconer, Assessment of array shape of tidal stream turbines on hydro-environmental impacts and power output, Renew. Energy 44 (2012) 318–327.
[12] B. Polagye, B. Van Cleeve, A. Copping, K. Kirkendall (Eds.), Environmental Effects of Tidal Energy Development, U.S. Dept. Commerce, vol. 116, NOAA Tech. Memo. F/SPO, 2011, p. 181.
[13] European Renewable Energy Council (EREC), Renewable Energy in Europe-Markets, Trends and Technologies, 2010.
[14] Eurostat, Share of Renewables in Energy Consumption in the EU Reached 17% in 2016, Eurostat Newsrelease, 2018, Accessed: 26 April 2018 http://ec.europa.eu/eurostat/documents/2995521/8612324/8-25012018-AP-EN.pdf/9d28caef-1961-4dd1-a901-af18f121fb2d.
[15] J.P. Sierra, D. González-Marco, J. Sospedra, X. Gironella, C. Mösso, A. Sánchez-Arcilla, Wave energy resource assessment in Lanzarote (Spain), Renew. Energy 55 (2013) 480–489.
[16] G. Iglesias, R. Carballo, Offshore and inshore wave energy assessment: Asturias (N Spain), Energy 35 (2010) 1964–1972.
[17] G. Iglesias, R. Carballo, Wave energy potential along the death coast (Spain), Energy 34 (2009) 1963, 197.
[18] I. Fairley, P. Evans, C. Woolridge, M. Willis, I. Masters, Evaluation of tidal stream resource in a potential array area via direct measurements, Renew. Energy 57 (2013) 70–78.
[19] J. Xia, R.A. Falconer, B. Lin, Numerical model assessment of tidal stream energy resources in the Severn Estuary, UK, In: Proc. Inst. Mech. Eng. Part a J. Power Energy, vol. 224, 2010, pp. 969–983.
[20] S. Draper, T. Adcock, A. Bothwick, G. Houlsby, Estimate of the tidal stream power resource of the Pentland Firth, Renew. Energy 63 (2014) 650–657.
[21] R.O. Murray, A. Gallego, A modelling study of the tidal stream resource of the Pentland Firth, Scotland, Renew. Energy 102 (2017) 326–340.
[22] D. Brooks, The hydrokinetic power resource in a tidal estuary: the Kennebec River of the central Maine coast, Renew. Energy 36 (2011) 1492–1501.
[23] B. Gunawan, V.S. Neary, J. Colby, Tidal energy site resource assessment in the East River tidal strait, near Roosevelt Island, New York, New York, Renew. Energy 71 (2014) 509–517.
[24] R.H. Karsten, J.M. McMillan, M.J. Lickley, R.D. Haynes, Assessment of tidal current energy in the Minas passage, Bay of Fundy, In: Proc. Inst. Mech. Eng. Part a J. Power Energy, vol. 222, 2008, pp. 493–507.
[25] M. Grabbe, E. Lalander, S. Lundin, M. Leijon, A review of the tidal current resource in Norway, Renew. Sustain. Energy Rev. 13 (2009) 1898–1909.
[26] A. Pacheco, Ó. Ferreira, R. Carballo, G. Iglesias, Evaluation of the production of tidal stream energy in an inlet channel by coupling field data and numerical modelling, Energy 71 (2014) 104–117.
[27] D. Li, S. Wang, P. Yuan, An overview of development of tidal current in China: energy resource conversion technology and opportunities, Renew. Sustain. Energy Rev. 14 (2010) 2896–2905.
[28] D.-S. Byun, D. Hart, W.-J. Jeong, Tidal current energy resources off the south and west coasts of Korea: preliminary observation-derived estimates, Energies 6 (2013) 566–578.
[29] L.S. Blunden, A.S. Bahaj, N.S. Aziz, Tidal current power for Indonesia? An initial resource estimation for the Alas Strait, Renew. Energy 49 (2013) 137–142.
[30] A. Rashid, Status and potentials of tidal in-stream energy resources in the southern coasts of Iran: a case study, Renew. Sustain. Energy Rev. 16 (2012) 6668–6677.
[31] R. Carballo, G. Iglesias, A. Castro, Numerical model evaluation of tidal stream energy resources in the ría de Muros (NW Spain), Renew. Energy 34 (2009) 1517–1524.
[32] V. Ramos, R. Carballo, M. Álvarez, M. Sánchez, G. Iglesias, A port towards energy self-sufficiency using tidal stream power, Energy 71 (2014) 432–444.
[33] M. deCastro, M. Gómez-Gesteira, R. Prego, R. Neves, Wind influence on water exchange between the Ría of Ferrol (NW Spain) and the shelf, Estuar. Coast Shelf Sci. 56 (2003) 1055–1064.
[34] M. deCastro, M. Gómez-Gesteira, R. Prego, I. Álvarez, Ría-ocean exchange driven by tides in the Ría of Ferrol (NW Spain), Estuar. Coast Shelf Sci. 61 (2004) 15–24.
[35] A. Cobelo-García, R. Prego, Inflluece of point sources on trace metal contamination and distribution in a semi-enclosed industrial embayment: the Ferrol Ría (NW Spain), Estuar. Coast Shelf Sci. 60 (2004) 695–703.
[36] A.F. Shchepetkin, J.C. McWilliams, The regional oceanic modeling system (ROMS): a split-explicit, free-surface, topography-following-coordinate oceanic model, Ocean Model. 9 (2005) 347–404.
[37] D.B. Haidvogel, H. Arango, W.P. Budgell, B.F. Cornuelle, E. Curchitser, E. Di Lorenzo, K. Fennel, W.R. Geyer, A.J. Hermann, L. Lanerolle, J. Levin, J.C. McWilliams, A.J. Miller, A.M. Moore, T.M. Powell, A.F. Shchepetkin, C.R. Sherwood, R.P. Signell, J.C. Warner, J. Wilkin, Ocean forecasting in terrain-following coordinates: formulation and skill assessment of the Regional Ocean modeling system, J. Comput. Phys. 227 (2008) 3595–3624.
[38] M.G. Sotillo, P. Cerralbo, P. Lorente, M. Grifoll, M. Espino, A. Sánchez-Arcilla, E. Álvarez-Fanjul, Coastal ocean forecasting in Spanish ports: the Samoa operational service, J. Oper. Oceanogr. (2018), (accepted with minor revisions).
[39] M.G. Sotillo, S. Cailleau, P. Lorente, B. Levier, R. Aznar, G. Reffray, A. Amo-Baladrón, J. Chanut, M. Benkiran, E. Alvarez-Fanjul, The MyOcean IBI ocean forecast and reanalysis systems: operational products and roadmap to the future Copernicus service, J. Oper. Oceanogr. 8 (2015) 63–79.
[40] G. Carter, M. Merrifield, Open boundary conditions for regional tidal simulations, Ocean Model. 18 (2007) 194–209.
[41] J.C. Warner, W.R. Geyer, J.A. Lerczak, Numerical modeling of an estuary: a comprehensive skill assessment, J. Geophys. Res. C Oceans 110 (2005) 1–13.
[42] S. Bahaj, A.F. Molland, J.R. Chaplin, W.M.J. Batten, Power and thrust measurements of marine current turbines under various hydrodynamic flow conditions in a cavitation tunnel and a towing tank, Renew. Energy 32 (2007) 407–426.
[43] L.S. Blunden, A.S. Bahaj, Tidal energy resource assessment for tidal stream generators, Proc. Inst. Mech. Eng. A-J Power Energy 221 (2007) 137–146.
[44] W.M.J. Batten, A.S. Bahaj, A.F. Molland, J.R. Chaplin, Experimentally validated numerical method for the hydrodynamic design of horizontal axis tidal turbines, Ocean Eng. 34 (2007) 1013–1020.
[45] R. Vennell, Exceeding the Betz limit with tidal turbines, Renew. Energy 55 (2013) 277–285.
[46] L. Myers, A.S. Bahaj, Simulated electrical power potential harnessed by marine current turbine arrays in the Alderney Race, Renew. Energy 30 (2005) 1713–1731.
[47] W-B. Chen, W.-C. Liu, M.-H. Hsu, Modeling assessment of tidal current energy at Kinmen Island, Taiwan, Renew. Energy 50 (2013) 1073–1082.

UNCORRECTED PROOF